Efficient Generation of Method of Moments Matrices Using Equivalent Dipole-Moment Method

Jiade Yuan, Changqing Gu, and Guodong Han

***Abstract*—In this letter, the equivalent dipole-moment (EDM) method is applied to compute the matrix elements of the method of moments (MoM) via solving the volume-surface integral equation (VSIE). Besides the advantage of reducing the calculation time significantly, this extended method is unnecessary to treat the boundary condition on the surface of dielectric body and easily constructed by using a simple procedure. The proposed approach can be applied if the distance between the source and the testing basis functions is beyond a threshold distance. Numerical results validate the efficiency and accuracy of the generated matrix elements, and the radar cross-section (RCS) has been verified.**

***Index Terms*—Electromagnetic scattering, equivalent dipole-moment (EDM), method of moments (MoM), radar cross-section (RCS).**

I. Introduction

METHOD OF MOMENTS (MoM) is a rigorous numerical solution method and has a broad application in computational electromagnetics field. However, traditional MoM incurs very high computational cost and memory requirements with the increasing of the electrical size for either surface integral equation (SIE) [1] or volume integral equation (VIE) [2]. This problem is extensively serious for the VIE since the entire dielectric volume needs to be meshed, resulting in more unknowns compared to the SIE. In addition, the conventional approaches to computing the MoM impedance matrix elements consume a considerable portion of the total solution time, and this, in turn, can place an inordinately heavy burden on the CPU regarding memory and time as the problem dimensions become large in terms of the wavelength. Fortunately, several efficient VIE-based or hybrid volume-surface integral equation (VSIE)-based methods have been studied in recent years, such as the multilevel fast multipole method (MLFMM) [3], the adaptive integral method (AIM) [4], the precorrected-FFT (P-FFT) method [5], the integral equation-QR (IE-QR) algorithm [6], the integral equation-FFT (IE-FFT) algorithm [7], and others are capable of overcoming this difficulty to some reasonable extent. However, most of the techniques mentioned rely upon iteration methods to solve large problems, and this can lead to convergence difficulties when dealing with objects with multiscale features.

More recently, the EDM method [8], [9] has been proposed to accelerate the direct solution of the MoM system of equations. In [8] and [9], the surface integral equation with Rao–Wilton–Glisson (RWG) [10] basis function is employed, and the metallic surfaces are discretized into triangular patches. Each RWG element is viewed as a dipole model so that the computation of impedance matrix elements is simplified significantly.

In this letter, the EDM method [8], [9] is extended and applied to analyze the composite conducting-dielectric objects via solving the VSIE with RWG and Schaubert–Wilton–Glisson (SWG) [2] basis function. The targets are discretized into triangular patches for metallic surfaces and tetrahedral cells for dielectric volume, respectively. The volume current (or surface current) distribution containing two adjacent tetrahedrons (or triangular patches) is replaced by an infinitesimal dipole with an equivalent dipole moment, shown in Fig. 1(a) and (b). Moreover, the tetrahedral boundary face on the surface of the dielectric body and its associated tetrahedron is also viewed as a dipole model, shown in Fig. 1(c), which make the conventional boundary condition treatments on dielectric surface unnecessary.

The article is organized as follows. Section II introduces the theory of the EDM method in detail, and Section III is shown the numerical results. The final section presents the conclusions.

II. Theory

In this section, we present the theoretical foundation of the procedure for efficient generation of MoM matrices associated with the coupled VSIE. The detailed derivation of the VSIE and the definition of RWG ($\mathbf{f}_{\rm sm}$) and SWG ($\mathbf{f}_{\rm vm}$) basis functions can be found in [2], [5], and [10]. The VSIE can be expressed as

$$\sum_{n=1}^{N_s} I_{\rm sn} Z_{mn}^{\rm ss} + \sum_{n=1}^{N_v} I_{vn} Z_{mn}^{\rm sv} = \langle \mathbf{E}^i, \mathbf{f}_{\rm sm} \rangle$$
$$\sum_{n=1}^{N_s} I_{\rm sn} Z_{mn}^{\rm vs} + \sum_{n=1}^{N_v} I_{\rm vn} Z_{mn}^{\rm vv} = \langle \mathbf{E}^i, \mathbf{f}_{\rm vm} \rangle \quad m = 1, 2, \cdots, N \quad (1)$$

where

$$Z_{mn}^{\rm ss} = -\langle \mathbf{E}_{\rm sn}^s, \mathbf{f}_{\rm sm}(\mathbf{r}) \rangle \quad (2)$$
$$Z_{mn}^{\rm sv} = -\langle \mathbf{E}_{vn}^s, \mathbf{f}_{sm}(\mathbf{r}) \rangle \quad (3)$$
$$Z_{mn}^{\rm vs} = -\langle \mathbf{E}_{sn}^s, \mathbf{f}_{vm}(\mathbf{r}) \rangle \quad (4)$$
$$Z_{mn}^{\rm vv} = \langle \mathbf{f}_{vn}(\mathbf{r}) / (j\omega\varepsilon(\mathbf{r}), \mathbf{f}_{vm}(\mathbf{r}) \rangle - \langle \mathbf{E}_{vn}^s, \mathbf{f}_{vm}(\mathbf{r}) \rangle \quad (5)$$

Manuscript received March 10, 2009; revised April 30, 2009. First published June 02, 2009; current version published July 21, 2009. This work was supported in part by the Aerospace Science Foundation of China (20070152001).

J. Yuan and C. Gu are with the College of Information Science and Technology, Nanjing University of Aeronautics and Astronautics, 210016 Nanjing, China (e-mail: yuanjd2010@yahoo.com.cn; gucq0138@sina.com).

G. Han is with Nanjing Research Institute of Electronics Technology, 210013 Nanjing, China (e-mail: guodong-han@nuaa.edu.cn.).

Digital Object Identifier 10.1109/LAWP.2009.2024337

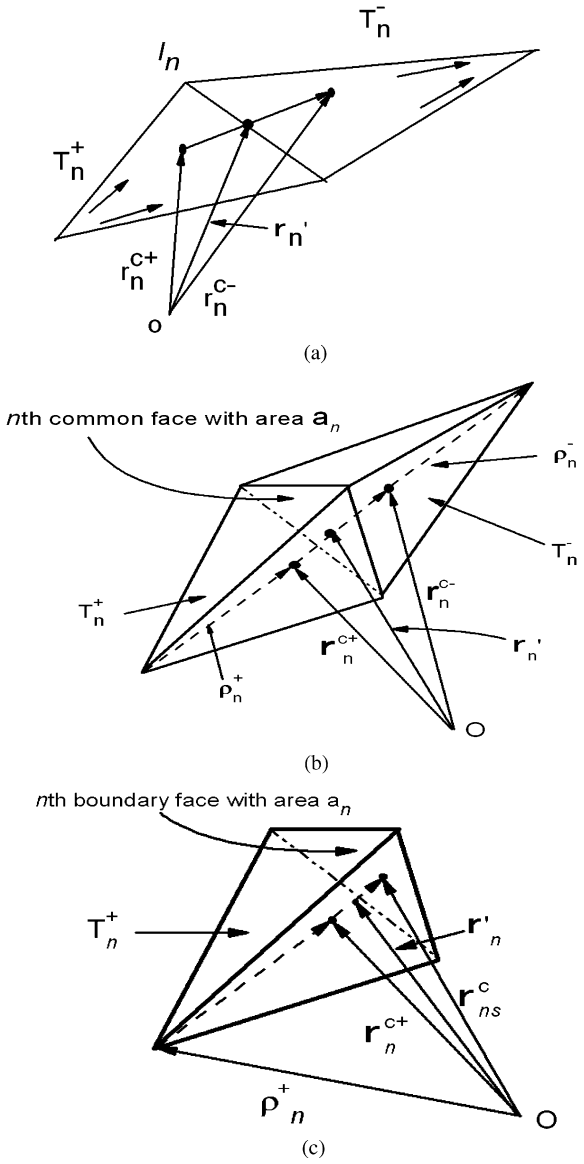

Fig. 1. (a) Pair of triangle patches with the nth common edge $l_{\rm n}$; (b) pair of tetrahedrons associated with the nth common face; (c) the nth boundary face associated with one tetrahedron.

where $Z_{mn}^{tu}(t = {\rm s,v}, u = {\rm s,v})$ stands for the impedance matrix element in row m and column n. $\mathbf{E}_{un}^{\rm s}(u = {\rm s,v})$ stands for the radiated electric field from the equivalent current of the nth RWG or SWG element.

On the conducting surface S, a RWG element n with two triangles $T_n^{\pm}$ adjacent to the edge of length l_n is shown in Fig. 1(a). The nth dipole moment $\mathbf{m}_{\rm s}$ is obtained by the integration of the surface current, corresponding to edge element n, over the element surface

$$\mathbf{m}_s = \int\limits_{T_n^+ + T_n^-} \mathbf{J}_{sn}(\mathbf{r}')ds' = I_{sn}\mathbf{m}_{sn} \tag{6}$$

where

$$\mathbf{m}_{sn} \approx l_n \left(\mathbf{r}_n^{c-} - \mathbf{r}_n^{c+}\right) \tag{7}$$

The dielectric body V, described by a SWG element n with two inner tetrahedrons $T_n^{\pm}$ adjacent to the common face of area a_n, is shown in Fig. 1(b). If the nth face is a boundary face, which is associated with only one tetrahedron, this corresponding tetrahedron is always assumed as T_n^+, as shown in Fig. 1(c). The nth dipole moment $\mathbf{m}_{\rm v}$ is obtained by the integration of the volume current, corresponding to face element n, over the element volume

$$\mathbf{m}_v = \int\limits_{T_n^+ + T_n^-} \mathbf{J}_{vn}(\mathbf{r}')dv' = I_{vn}\mathbf{m}_{vn} \tag{8}$$

where

$$\mathbf{m}_{vn} \approx \begin{cases} a_n\kappa(\mathbf{r})\left(\mathbf{r}_n^{c-} - \mathbf{r}_n^{c+}\right), & T_n^{\pm} \in V \\ a_n\kappa(\mathbf{r})\left(\mathbf{r}_{ns}^{c} - \mathbf{r}_n^{c+}\right), & T_n^{+} \in V \text{ and } T_n^{-} \notin V. \end{cases} \tag{9}$$

Here, the dielectric material of each dipole model is assumed uniform. The $\mathbf{r}_n^{c-}$, $\mathbf{r}_n^{c+}$ and $\mathbf{r}_{ns}^{c}$ are the centroid radius vector of T_n^+, T_n^-, and the nth boundary face, respectively, as shown in Fig. 1.

Referring to [8] and [9], the radiated electric fields of the nth infinitesimal dipole at the field point $\boldsymbol{r}$ can be expressed as

$$\mathbf{E}_{un}^{\rm s}(\mathbf{r}) = \frac{\eta}{4\pi}\left[(\mathbf{M}_{un} - \mathbf{m}_{un})\left(\frac{jk}{R} + C\right) + 2\mathbf{M}_{un}C\right] \times e^{-jkR} \quad u = {\rm s,v} \tag{10}$$

in which

$$C = \frac{1}{R^2}\left[1 + \frac{1}{jkR}\right] \tag{11}$$

and

$$\mathbf{M}_u = \frac{(\mathbf{R}\cdot\mathbf{m}_u)\mathbf{R}}{R^2} \tag{12}$$

where $\mathbf{R} = \mathbf{r} - \mathbf{r}'$ and $R = |\mathbf{R}|$. Equation (10) is the exact expressions and valid at arbitrary distances from the dipole, not only in the far-field. However, if the observation point is close to the dipole for a separation distance of less than a threshold distance between the source and the testing function locations, the SWG or RWG element cannot be regarded as an infinitesimal dipole model, so (10) will not hold. In this case, the conventional MoM is still used to calculate the impedance matrix element; otherwise, the MoM matrix elements are computed by the EDM method directly.

On the basis of extensive numerical experimentation, we find that $0.15\lambda_0$ (λ_0 is the wavelength in free-space) is an appropriate threshold distance for the triangle patches when the edge length of triangles is less than $\lambda_0/10$, which is also in accordance with [9]. At the same time, $0.15\lambda_{\rm g}$ ($\lambda_{\rm g}$ is the wavelength in dielectric) is an appropriate threshold distance for the tetrahedral cells when the edge length of the tetrahedron is less than $\lambda_{\rm g}/10$. When setting up the discretized model of a target, the surface patches should coincide with the external faces of the volume cells on the conductor-dielectric interface—namely, partial overlap is not permitted. Therefore, $\lambda_{\rm g}/10$ and $0.15\lambda_{\rm g}$ are chosen as the maximum edge length and

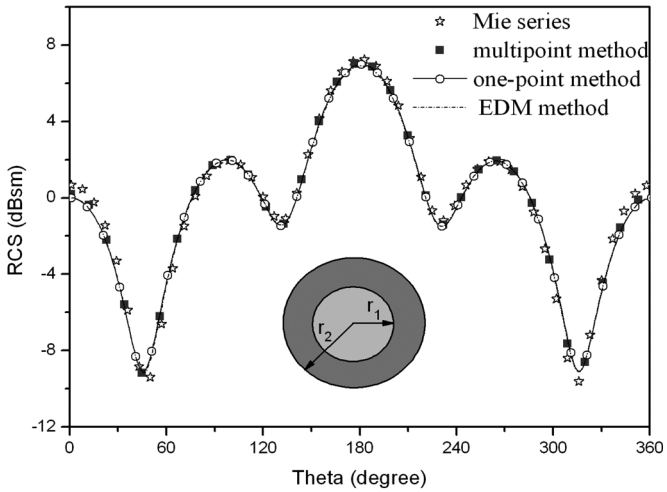

Fig. 2. Bistatic RCS ($\theta\theta$ polarization) of a conducting sphere ($\mathrm{r}_1 = 0.3$ m) with a dielectric coating ($\mathrm{r}_2 = 0.4$ m, $\varepsilon_\mathrm{r} = 3$).

TABLE I
TOTAL CPU TIME AND IMPEDANCE MATRIX FILLING TIME OF MULTIPOINT INTEGRATION, ONE-POINT INTEGRATION IN FAR-FIELD, AND EDM METHOD

	Four-point	One-point	EDM method
Total time (s)	1532	810	731
Filling time (s)	986	266	187

the threshold distance, respectively, for both RWG triangles and SWG tetrahedral cells in this letter.

Substituting (10) into (2)–(5) and referring to [2] and [10], the expressions of the impedance matrix element $Z_{m,n}$ are calculated by

$$Z_{m,n} \approx \begin{cases} -l_m\left[e^{-jkR}\mathbf{E}^s_{un}(R)|_{R=|\mathbf{r}'_m-\mathbf{r}'_n|} \cdot(\mathbf{r}^{c-}_m-\mathbf{r}^{c+}_m)\right] & T^{\pm}_m \in S \\ -a_m\left[e^{-jkR}\mathbf{E}^s_{un}(R)|_{R=|\mathbf{r}'_m-\mathbf{r}'_n|} \cdot(\mathbf{r}^{c-}_m-\mathbf{r}^{c+}_m)\right] & T^{\pm}_m \in V \\ -a_m\left[e^{-jkR}\mathbf{E}^s_{un}(R)|_{R=|\mathbf{r}'_m-\mathbf{r}'_n|} \cdot(\mathbf{r}^{c}_{ms}-\mathbf{r}^{c+}_m)\right] & T^{+}_m \in V \text{ and } T^{-}_m \notin V \end{cases} \tag{13}$$

where the $\mathbf{r}^{c-}_m$, $\mathbf{r}^{c+}_m$, and $\mathbf{r}^{c}_{m\mathrm{s}}$ are the centroid radius vector of T^+_m, T^-_m, and the mth face, respectively. $\mathbf{r}'_n$ and $\mathbf{r}'_m$ are the center radius vector of the nth and the mth equivalent dipole model, respectively

$$\mathbf{r}'_u = \begin{cases} (\mathbf{r}^{c+}_u + \mathbf{r}^{c-}_u)/2, & T^{\pm}_u \in V, S \\ (\mathbf{r}^{c+}_u + \mathbf{r}^{c}_{us})/2, & T^{+}_u \in V \text{ and } T^{-}_u \notin V \end{cases} \qquad u = m, n. \tag{14}$$

The far-field approximations of the scattering electric field are used and the RCS can be expressed as

$$\mathrm{RCS} = \sum_{n=1}^{N} \frac{k^2\eta^2}{4\pi}\left|I_n(\mathbf{M}_n - \mathbf{m}_n)\cdot e^{jk\mathbf{r}'_n\cdot\mathbf{u}}\right|^2 \tag{15}$$

where

$$\mathbf{u} = \mathbf{u}_x \sin\theta\cos\varphi + \mathbf{u}_y \sin\theta\sin\varphi + \mathbf{u}_z\cos\theta. \tag{16}$$

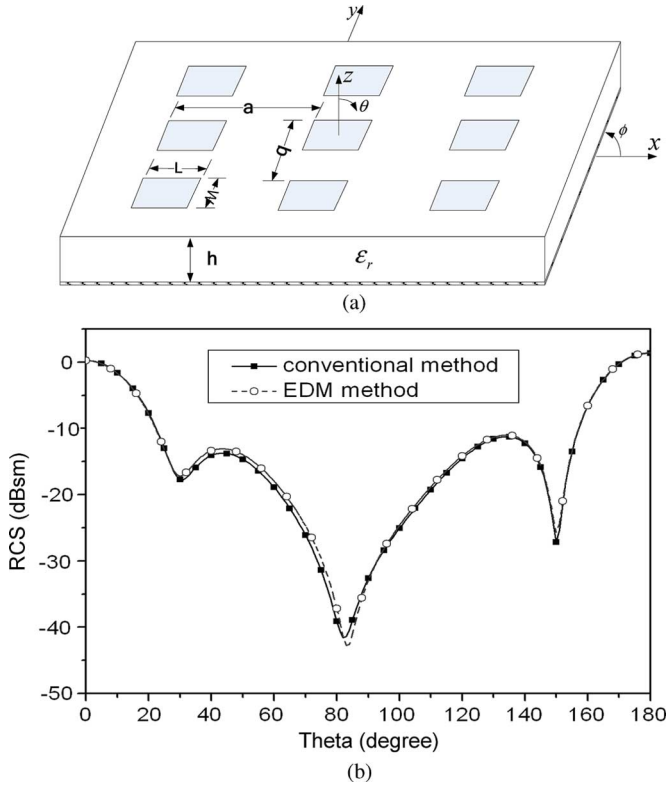

Fig. 3. (a) Geometry of a 3×3 array of rectangular microstrip patches on a finite grounded dielectric substrate. (patch size: $\mathrm{L} = 36.6$ mm $\mathrm{W} = 26$ mm, $\mathrm{a} = \mathrm{b} = 55.517$ mm, $\varepsilon_\mathrm{r} = 2.17$, substrate thickness: $\mathrm{h} = 1.58$ mm). (b) Bistatic RCS ($\theta\theta$ polarization) versus θ at normal incidence ($\theta_{inc} = 180°$, $\varphi_{inc} = 0°$).

III. NUMERICAL RESULTS

In the traditional MoM, we usually choose a multipoint integration for the near-field interactions and a one-point integration for the far-field interactions ($0.15\lambda_\mathrm{g}$ or further) to generate the impedance matrix. In the following examples, the EDM method for efficient MoM matrix generation is applied to calculate the bistatic RCS. The simulation results are given for comparison to the traditional MoM ones to validate the efficiency and accuracy of this equivalent method. All the tests are run on a processor with 3.2-GHz CPU speed.

We first consider a conducting sphere covered by a dielectric shell (radii: $\mathrm{r}_1 = 0.3$ m, $\mathrm{r}_2 = 0.4$ m, $\varepsilon_\mathrm{r} = 3$, incident angle: $\theta_\mathrm{inc} = 180°$, $\varphi_\mathrm{inc} = 0°$, incident frequency: 300 MHz), as shown in the inset of Fig. 2. The surface of the conducting sphere is discretized into 318 triangular patches, and the volume of the dielectric shell into 2343 tetrahedrons, yielding a total number of 5655 unknowns. Fig. 2 gives the bistatic RCS curves obtained from the one-point integration, the multipoint integration (three integration points in triangle patches and four integration points in tetrahedrons) in the far-field, the EDM method, and the Mie series method. It is found that our results agree well with the Mie series method, which is the exact solution and used as a reference. The CPU time and the impedance matrix filling time of each method are listed in Table I. Compared to the one-point integration in far-field, the EDM method yields a reduction of about 30% in filling time to the impedance matrix.

In the second example, we consider the plane-wave scattering from a finite 3×3 array of microstrip patch antennas. The geometric parameters are taken from [11] (patch size: 36.6 mm $\times$ 26 mm, $\varepsilon_{\rm r} = 2.17$, substrate thickness: $h = 1.58$ mm), and the ground plane size is 166.6 mm $\times$ 166.6 mm. The distance between two adjacent elements in both the x and$y$ directions is 55.517 mm, as shown in Fig. 3(a). The array objects are discretized into 6808 tetrahedrons and 4257 triangles, respectively, yielding a total of 20 258 unknowns. The incident wave is along the direction of $\theta_{\rm inc} = 180^\circ$ and $\varphi_{\rm inc} = 0^\circ$, and the bistatic RCS at 3.7 GHz is given in Fig. 3(b). Good agreement is observed between the conventional method and the EDM method. The total CPU time is 16 315 s in conventional method and 7347 s in the EDM method respectively, which yields a reduction of about 55% in CPU time.

Through the comparison of example 1 and 2, we find that the computational efficiency of the EDM method is higher compared to the traditional one-point integration MoM method with the increase of the electrical size of the target.

IV. Conclusion

The EDM method has been successfully applied to the acceleration of the impedance matrix filling in the MoM matrices via solving VSIE. It is demonstrated that all of the matrix elements satisfying a minimum distance criterion for separation between the source and testing basis functions can be represented in terms of the EDM method. The application of the EDM method significantly reduces the computational complexity of the impedance matrix as well as the CPU time. The proposed method is based on the physics properties and is easily constructed by using a simple procedure, so it is suitable to be applied in many different MoM-based approaches for the analysis of arbitrarily shaped composite conducting-dielectric objects.

Acknowledgment

The authors gratefully acknowledge the help of Dr. L. Zhuo at Nanjing University of Aeronautics and Astronautics, without whose help and advice the letter could not be accomplished.

References

[1] S. M. Rao, C. C. Cha, R. L. Cravey, and D. L. Wilkes, "Electromagnetic scattering from arbitrary shaped conducting bodies coated with lossy materials of arbitrary thickness," *IEEE Trans. Antennas Propag.*, vol. 39, no. 5, pp. 627–631, May 1991.

[2] D. H. Schaubert, D. R. Wilton, and A. W. Glisson, "A tetrahedral modeling method for electromagnetic scattering by arbitrarily shaped inhomogeneous dielectric bodies," *IEEE Trans. Antennas Propag.*, vol. AP-32, no. 1, pp. 77–85, Jan. 1984.

[3] K. Sertel and J. L. Volakis, "Multilevel fast multipole method solution of volume integral equations using parametric geometry modeling," *IEEE Trans. Antennas Propag.*, vol. 52, no. 7, pp. 1686–1691, Jul. 2004.

[4] D. Z. Zhang and Q. H. Lin, "A volume adaptive integral method (VAIM) for 3-D inhomogeneous objects," *IEEE Antenna Wireless Propag. Lett.*, vol. 1, pp. 102–105, 2002.

[5] X. C. Nie, L. W. Li, N. Yuan, T. S. Yeo, and Y. B. Gan, "A fast volume-surface integral equation solver for scattering from composite conducting-dielectric objects," *IEEE Trans. Antennas Propag.*, vol. 53, no. 2, pp. 818–824, Feb. 2005.

[6] N. A. Ozdemir and J. F. Lee, "A low-rank IE-QR algorithm for matrix compression in volume integral equations," *IEEE Trans. Magn.*, vol. 40, no. 2, pp. 1017–1020, Mar. 2004.

[7] N. A. Ozdemir and J. F. Lee, "IE-FFT algorithm for a nonconformal volume integral equation for electromagnetic scattering from dielectric objects," *IEEE Trans. Magn.*, vol. 44, no. 6, pp. 1398–1401, Mar. 2008.

[8] S. N. Makarov, *Antenna and EM Modeling With MATLAB*. New York: Wiley, 2002.

[9] J. S. Y. Köksoy, V. V. S. Prakash, and R. Mittra, "Efficient generation of method of moments matrices using the characteristic function method," *IEEE Trans. Antennas Propag.*, vol. 52, no. 12, pp. 3405–3410, Dec. 2004.

[10] S. M. Rao, D. R. Wilton, and A. W. Glisson, "Electromagnetic scattering by surfaces of arbitrary shape," *IEEE Trans. Antennas Propag.*, vol. AP-30, no. 3, pp. 409–418, May 1982.

[11] C. F. Wang, F. Ling, and J. M. Jin, "A fast full-wave analysis of scattering and radiation from large finite arrays of microstrip antennas," *IEEE Trans. Antennas Propag.*, vol. 46, no. 10, pp. 1467–1474, Oct. 1998.